

Data-Driven Meets Geometric Control: Zero Dynamics, Subspace Stabilization, and Malicious Attacks

Federico Celi¹, Graduate Student Member, IEEE, and Fabio Pasqualetti¹, Member, IEEE

Abstract—Studying structural properties of linear dynamical systems through invariant subspaces is one of the key contributions of the geometric approach to system theory. In general, a model of the dynamics is required in order to compute the invariant subspaces of interest. In this letter we overcome this limitation by finding direct data-driven formulas for some of the foundational tools of the geometric approach. We use our results to (i) find a feedback gain that confines the system state within a subspace, (ii) compute the invariant zeros of the unknown system, and (iii) design attacks that remain undetectable.

Index Terms—Linear feedback control systems, algebra, big data applications, fault tolerant control.

I. INTRODUCTION

THE GEOMETRIC approach is a collection of notions and algorithms for the analysis and control of dynamical systems. Differently from the classic methods in the frequency and state space domains [1], the geometric approach offers an intuitive and coordinate-free analysis of the properties of dynamical systems in terms of appropriately defined subspaces, and synthesis algorithms based on subspace operations, such as sum, intersection, and orthogonal complementation. The geometric approach has been successfully used to solve a variety of complex control and estimation problems; we refer the interested reader to [2] for a detailed treatment of the main geometric control notions and their applications.

Similarly to the frequency and state-space approaches to control, the geometric approach assumes an accurate, in fact exact, representation of the system dynamics. To overcome this limitation and in response to an ever-increasing availability of sensors, historical data, and machine learning algorithms, the behavioral approach, and more generally a data-driven approach, has seen a rapid increase in popularity. Here, system

analysis and control synthesis do not require a model of the dynamics and are instead obtained directly from experimental data reflecting the system dynamics [3].

While analysis, control and estimation problems can often be solved equivalently using different methods, the frequency, state-space, geometric, and data-driven approaches all offer complementary insights into the structure and properties of the system dynamics, and together contribute to forming a comprehensive theory of systems. In this letter we create the first connections between the geometric and data-driven approaches to system analysis and control. In particular, we derive data-driven expressions of the fundamental sets used in the geometric approach to solve a variety of control and estimation problems, and show how these sets have an even more insightful and straightforward interpretation when analyzed in the higher-dimensional data space as compared to their geometric view in the lower-dimensional state space.

Related work: From the first definitions of controlled and conditioned invariant subspaces, the geometric approach to control has evolved over the last decades into a full theory and a set of algorithms for linear [2] and nonlinear [4] systems. Applications of the geometric approach include the disturbance decoupling [5] and fault detection [6] problems, the characterization of stealthy attacks in cyber-physical systems [7], and the secure state estimation problem [8].

The data-driven approach to system analysis and control is receiving renewed and increased interest. While traditional indirect data-driven methods use data to identify a model of the system [9] and proceed to synthesize a controller in a second step, direct data-driven methods bypass (at least apparently [10]–[12]) the identification step and design control actions directly from data. In this framework, recent results tackle various problems for linear systems, including optimal [13], [14], robust [15] and distributed [16]–[19] control, as well as unknown-input estimation [20]. We refer the reader to [21] for a recent survey on data-driven control.

Main contributions of this letter: First, for the linear, discrete, time-invariant systems described by the triple (A, B, C) , we derive explicit, closed-form data-driven expressions of (i) \mathcal{V}^* , the largest $(A, \text{Im}(B))$ -controlled invariant subspace contained in $\text{Ker}(C)$, (ii) \mathcal{S}^* , the smallest $(A, \text{Ker}(C))$ -conditioned invariant subspace containing $\text{Im}(B)$, (iii) the feedback gain F such that $(A + BF)\mathcal{V}^* \subseteq \mathcal{V}^*$, and (iv) the invariant zeros

Manuscript received January 10, 2022; revised March 28, 2022; accepted April 15, 2022. Date of publication April 27, 2022; date of current version May 4, 2022. This work supported in part by the Air Force Office of Scientific Research (AFOSR) under Award FA9550-20-1-0140 and Award FA9550-19-1-0235, and in part by the Army Research Office (ARO) under Award W911NF2020267(NC4). Recommended by Senior Editor L. Menini. (Corresponding author: Federico Celi.)

The authors are with the Department of Mechanical Engineering, University of California at Riverside, Riverside, CA 92521 USA (e-mail: fceli@engr.ucr.edu; fabiopas@engr.ucr.edu).

Digital Object Identifier 10.1109/LCSYS.2022.3170866

of (A, B, C) . Since \mathcal{V}^* and \mathcal{S}^* are the basis of the geometric approach developed in [2], our data-driven formulas constitute the basis of a data-driven and model-free theory of geometric control. Second, our results show that the fundamental invariant subspaces of the geometric approach, which are often computed recursively when operating in the state space, have a simple and direct interpretation in the higher-dimensional data space, where they can be computed by solving appropriately defined sets of linear equations. Third, we demonstrate the utility of our formulas to design undetectable data-driven attacks.

Paper organization: Section II contains our problem setup and some preliminary notions. Section III contains our data-driven formulas of the fundamental invariant subspaces of the geometric approach. Finally, Sections IV and V contain our illustrative examples and conclusion, respectively.

Notation: We follow the notation of [2]. The rank, null space, transpose, and Moore-Penrose pseudoinverse of the real matrix $A \in \mathbb{R}^{n \times m}$ are denoted with $\text{rank}(A)$, $\text{Ker}(A)$, A^\top , and A^\dagger respectively. We use $\{0\}$ to denote the trivial subspace containing only the origin. Given a matrix A and a subspace \mathcal{V} of appropriate dimensions, $A^{-1}\mathcal{V}$ denotes the pre-image of \mathcal{V} by the, possibly singular, matrix A . $V = \text{Basis}(\mathcal{V})$ denotes any full-column rank matrix such that $\text{Im}(V) = \mathcal{V}$. The Kronecker product between matrices A and B is denoted by $A \otimes B$ [22].

II. PROBLEM SETUP AND PRELIMINARY NOTIONS

We consider the discrete-time linear time-invariant system

$$x(t+1) = Ax(t) + Bu(t) \quad (1a)$$

$$y(t) = Cx(t) \quad (1b)$$

where $x \in \mathbb{R}^n$, $u \in \mathbb{R}^m$ and $y \in \mathbb{R}^p$ are the state, input and output vectors, respectively, and (A, B, C) are constant matrices of appropriate dimensions. For any horizon $T \geq 1$, the state and output trajectories of (1) can be written as

$$\begin{bmatrix} x(1) \\ x(2) \\ \vdots \\ x(T) \end{bmatrix} = \begin{bmatrix} A \\ A^2 \\ \vdots \\ A^T \end{bmatrix} x(0) + \underbrace{\begin{bmatrix} B & \cdots & 0 & 0 \\ AB & \cdots & 0 & 0 \\ \vdots & \ddots & \vdots & \vdots \\ A^{T-1}B & \cdots & AB & B \end{bmatrix}}_{F_T^x} \underbrace{\begin{bmatrix} u(0) \\ u(1) \\ \vdots \\ u(T-1) \end{bmatrix}}_{U_T}, \quad (2)$$

and

$$\begin{bmatrix} y(0) \\ y(1) \\ \vdots \\ y(T-1) \end{bmatrix} = \begin{bmatrix} C \\ CA \\ \vdots \\ CA^{T-1} \end{bmatrix} x(0) + \underbrace{\begin{bmatrix} 0 & \cdots & 0 & 0 \\ CB & \cdots & 0 & 0 \\ \vdots & \ddots & \vdots & \vdots \\ CA^{T-2}B & \cdots & CB & 0 \end{bmatrix}}_{F_T^y} U_T. \quad (3)$$

Throughout this letter, we assume that the system matrices are not known and base our approach on a set of prerecorded trajectories obtained by arbitrarily probing the system (1).

A. Data Collection

Data is collected from a set of N open-loop control experiments with horizon T and consist of the state and output trajectories obtained from (1) with initial condition x_0^i and

control sequence U_T^i , for $i \in \{1, \dots, N\}$. In particular, when needed, the following data matrices will be used:¹

$$X = [X_T^1 \quad \cdots \quad X_T^N] \in \mathbb{R}^{nT \times N}, \quad (4a)$$

$$X_0 = [x^1(0) \quad \cdots \quad x^N(0)] \in \mathbb{R}^{n \times N}, \quad (4b)$$

$$X_F = [x^1(T) \quad \cdots \quad x^N(T)] \in \mathbb{R}^{n \times N}, \quad (4c)$$

$$Y = [Y_T^1 \quad \cdots \quad Y_T^N] \in \mathbb{R}^{pT \times N}, \quad (4d)$$

$$U = [U_T^1 \quad \cdots \quad U_T^N] \in \mathbb{R}^{mT \times N}. \quad (4e)$$

From (2)-(3), we note the following relationships:

$$\begin{bmatrix} X \\ Y \end{bmatrix} = \begin{bmatrix} O_T^x & F_T^x \\ O_T^y & F_T^y \end{bmatrix} \begin{bmatrix} X_0 \\ U \end{bmatrix}. \quad (5)$$

We make the following assumption of persistently-exciting experimental inputs, which is generically satisfied by choosing the inputs and initial states independently and randomly.

Assumption 1: The experimental inputs and initial conditions are persistently exciting, that is,

$$\text{rank} \begin{bmatrix} X_0 \\ U \end{bmatrix} = n + mT. \quad (6)$$

Let $K_0 = \text{Basis}(\text{Ker}(X_0))$ and $K_U = \text{Basis}(\text{Ker}(U))$. Assumption 1 ensures that $X_0 K_U$ and $U K_0$ are full-row rank, respectively. Assumption 1 is a standard assumption in data driven studies [12], [15], and places a lower bound on the number of experiments $N \geq n + mT$.

Remark 1 (Alternative data-driven representations): Different data formats can be used to obtain a non-parametric data-driven representation of the system (1), including our representation (4) as well as Hankel and Page matrices [12], [15]. While Hankel and Page matrices are generated from a single controlled trajectory, the matrices in (4) can be obtained from a single controlled trajectory or from a collection of shorter controlled trajectories. Different data collections can be more convenient for the solution of different problems, with, currently, Hankel and Page matrices being used mostly for feedback control problems [15] and multiple trajectories for robustness problems [13].

B. Controlled and Conditioned Invariant Subspaces

The notions of controlled and conditioned invariant subspaces are the basis of the geometric approach for the analysis and control of linear systems. We now recall their definition and basic properties. We refer the interested reader to [2], [23], [24] for a detailed treatment of this subject.

Definition 1 ((A, B)-controlled invariant): Given a matrix $A \in \mathbb{R}^{n \times n}$ and a subspace $\mathcal{B} \subseteq \mathbb{R}^n$, a subspace $\mathcal{V} \subseteq \mathbb{R}^n$ is an (A, \mathcal{B}) -controlled invariant subspace if

$$A\mathcal{V} \subseteq \mathcal{V} + \mathcal{B}. \quad (7)$$

When $\mathcal{B} = \text{Im}(B)$, the notion of controlled invariance refers to the possibility of confining the state trajectory of the system (1) within a subspace. Specifically, the subspace \mathcal{V} is an $(A, \text{Im}(B))$ -controlled invariant subspace if, for every initial state in \mathcal{V} , there exists a control input such that the state belongs to \mathcal{V} at all times. Of particular interest is \mathcal{V}^* ,

¹The matrices (4) are used for our derivations. However, our results depend often only on a subset of these data matrices.

the largest $(A, \text{Im}(B))$ -controlled invariant subspace contained in $\text{Ker}(C)$. The subspace \mathcal{V}^* contains all trajectories of (1) that generate an identically zero output. Hence, it holds that $\mathcal{V}^* = \{0\}$ if and only if the system (1) features no invariant zeros, a notion that is at the basis of the analysis of stealthy attacks and unknown-input observers [7], among others.

Definition 2 ((A, C)-conditioned invariant): Given a matrix $A \in \mathbb{R}^{n \times n}$ and a subspace $\mathcal{C} \subseteq \mathbb{R}^n$, a subspace $\mathcal{S} \subseteq \mathbb{R}^n$ is an (A, \mathcal{C}) -conditioned invariant subspace if

$$A(\mathcal{S} \cap \mathcal{C}) \subseteq \mathcal{S}. \quad (8)$$

When $\mathcal{C} = \text{Ker}(C)$, the notion of conditioned invariance arises in the context of state estimation. Specifically, the subspace \mathcal{S} is an $(A, \text{Ker}(C))$ -conditioned invariant subspace if it is possible to design an (asymptotic) observer that reconstructs the state up to a canonical projection onto $\mathbb{R}^n \setminus \mathcal{S}$ by processing the initial condition, the input, and the measurements of the system (1). Of particular interest is \mathcal{S}^* , the smallest $(A, \text{Ker}(C))$ -conditioned invariant subspace containing $\text{Im}(B)$. In fact, the orthogonal complement of \mathcal{S}^* is the largest subspace that can be estimated with a dynamic observer in the presence of an unknown input.

The subspaces \mathcal{V}^* and \mathcal{S}^* can be conveniently computed using simple recursive algorithms [2]. Further, these subspaces can be used to characterize important properties of the system (1). For instance, the system (1) is right invertible if and only if $\mathcal{V}^* \cup \mathcal{S}^* = \mathbb{R}^n$, and left invertible if and only if the subspace $\mathcal{R}^* = \mathcal{V}^* \cap \mathcal{S}^*$ is the trivial subspace [2]. It should be noticed that \mathcal{R}^* coincides with the largest subspace that can be reached from the origin with trajectories that belong to \mathcal{V}^* at all times (hence, generating an identically zero output).

The definition of the subspaces \mathcal{V}^* , \mathcal{S}^* and \mathcal{R}^* , as well as the algorithms to compute them, assume the exact knowledge of the system matrices. Instead, in the remainder of this letter we derive purely data-driven expressions of these subspaces, which also offer an alternative interpretation of them. Similarly to how \mathcal{V}^* , \mathcal{S}^* and \mathcal{R}^* are used in the geometric approach, our data-driven formulas can also be used to solve a variety of estimation and control problems.

III. DATA-DRIVEN GEOMETRIC CONTROL

We begin with finding a data-driven expression of the subspace \mathcal{V}^* for the system (1), the largest $(A, \text{Im}(B))$ -controlled invariant subspace contained in $\text{Ker}(C)$.

Theorem 1 (Data driven formula for \mathcal{V}^):* Let X_0 and Y be as in (4b) and (4d), respectively, with $T \geq n$. Then,

$$\mathcal{V}^* = X_0 \text{Ker}(Y). \quad (9)$$

Notice that (9) requires only the knowledge of the initial state X_0 and the output trajectory Y of N experiments in (4). To prove Theorem 1, recall that \mathcal{V}^* is the set of initial states for which there exists a control input such that the resulting state trajectory generates an identically zero output. Since the system is linear, under our assumption of persistently exciting experimental inputs, any system trajectory can be expressed as an appropriate linear combination of the experimental trajectories. We next formalize this intuition.

Lemma 1 (Data-driven trajectories of (1)): Let (4) be the data generated by the system (1) with $T \geq n$. Let \bar{X}_T and \bar{Y}_T be the state and output trajectories of (1) generated with some initial condition and control input. Then,

$$\begin{bmatrix} \bar{X}_T \\ \bar{Y}_T \end{bmatrix} = \begin{bmatrix} XK_U & XK_0 \\ YK_U & YK_0 \end{bmatrix} \begin{bmatrix} \alpha \\ \beta \end{bmatrix}, \quad (10)$$

for some vectors α and β .

Proof: Let \bar{x}_0 and \bar{U}_T be the initial condition and input to (1). Since the matrices X_0K_U and UK_0 are full-row rank (see Assumption 1), there exists α and β such that

$$\bar{x}_0 = X_0K_U\alpha \quad \text{and} \quad \bar{U}_T = UK_0\beta. \quad (11)$$

From (2) we have

$$\begin{aligned} \bar{X}_T &= O_T^X \bar{x}_0 + F_T^X \bar{U}_T = O_T^X X_0K_U\alpha + F_T^X UK_0\beta \\ &= XK_U\alpha + XK_0\beta, \end{aligned}$$

where the last equality follows from (5). Similarly from (3),

$$\begin{aligned} \bar{Y}_T &= O_T^Y \bar{x}_0 + F_T^Y \bar{U}_T = O_T^Y X_0K_U\alpha + F_T^Y UK_0\beta \\ &= YK_U\alpha + YK_0\beta, \end{aligned}$$

which concludes the proof. \blacksquare

Lemma 1 shows how any state and output trajectory of (1) can be written as a linear combination of the available data. In particular, state and output trajectories are obtained in (10) as the sum of the free and forced responses, which are reconstructed from data of arbitrary control experiments. In fact, $XK_U\alpha$ is the state trajectory of (1) with initial condition $X_0K_U\alpha$ and zero input (free response), while $XK_0\beta$ is the state trajectory of (1) with zero initial condition and input $UK_0\beta$ (forced response). We remark that Assumption 1 of persistently exciting inputs is necessary to obtain this result.

The following instrumental Lemma shows that it is sufficient to consider trajectories of any finite length $T \geq n$ to compute \mathcal{V}^* , and is instrumental to the proof of Theorem 1.

Lemma 2 (Computing \mathcal{V}^ from trajectories of finite length):* For the system (1), any initial state x_0 , and any finite horizon $T \geq n$, the following statements are equivalent:

- (i) $x_0 \in \mathcal{V}^*$;
- (ii) there exists an input sequence $u(0), \dots, u(T-1)$ such that $y(t) = 0$ for all $t \in \{0, \dots, T-1\}$.

Proof:

(i) \Rightarrow (ii) Follows from the definition of \mathcal{V}^* .

(ii) \Rightarrow (i) Notice that $y(T-1) = Cx(T-1) = 0$. Thus, $x(T-1) \in \text{Ker}(C) = \mathcal{V}_0$. Similarly, $x(T-2)$ satisfies

$$x(T-1) = Ax(T-2) + Bu(T-2), \quad \text{and}$$

$$y(T-2) = Cx(T-2) = 0.$$

This implies that

$$\begin{aligned} x(T-2) &\in A^{-1}(x(T-1) - Bu(T-2)) \\ &\subseteq A^{-1}(\mathcal{V}_0 + \text{Im}(B)) \cap \text{Ker}(C) = \mathcal{V}_1 \end{aligned}$$

Iterating this procedure yields

$$x(T-1) \in \mathcal{V}_0 = \text{Ker}(C), \quad \text{and} \quad (12a)$$

$$x(T-i) \in \mathcal{V}_i = A^{-1}(\mathcal{V}_{i-1} + \text{Im}(B)) \cap \text{Ker}(C). \quad (12b)$$

Since \mathcal{V}_i converges to \mathcal{V}^* is at most n steps [2], we have that $x(T - \tau) \in \mathcal{V}^*$ for all $\tau \geq n$, which concludes the proof. ■

We now prove Theorem 1 using Lemma 1 and 2.

Proof of Theorem 1: From Lemma 2 we seek all initial conditions x_0 for which the output can be maintained at zero for $T \geq n$ steps. From (10), the vectors α and β that identify state trajectories with identically zero output must satisfy

$$\begin{bmatrix} \alpha \\ \beta \end{bmatrix} \in \text{Ker}[YK_U \quad YK_0]. \quad (13)$$

The initial condition corresponding to such trajectories is $x_0 = X_0 K_U \alpha$ (11). Thus, using (13), \mathcal{V}^* becomes $\mathcal{V}^* = [X_0 K_U \quad 0] \text{Ker}[YK_U \quad YK_0] = X_0 \text{Ker}(Y)$. The last equality follows from some algebraic manipulations, that are here omitted. ■

We next find a data-driven expression for \mathcal{S}^* , the smallest $(A, \text{Ker}(C))$ conditioned invariant containing $\text{Im}(B)$.

Theorem 2 (Data driven formula for \mathcal{S}^):* Let X_0, X_F and Y be as in (4b), (4c) and (4d), respectively, with $T \geq n$. Then,

$$\mathcal{S}^* = X_F K_0 \text{Ker}(YK_0). \quad (14)$$

To prove Theorem 2, we first show that, similarly to the case of \mathcal{V}^* , the subspace \mathcal{S}^* can be computed from a collection of trajectories of finite length $T \geq n$.

Lemma 3 (Computing \mathcal{S}^ from trajectories of finite length):* For the system (1) and any finite horizon $T \geq n$, the following statements are equivalent:

- (i) $x(T) \in \mathcal{S}^*$;
- (ii) there exists an input sequence $u(0), \dots, u(T-1)$ such that $y(t) = 0$ for all $t \in \{0, \dots, T-1\}$ and $x(0) = 0$.

Proof:

(i) \Rightarrow (ii) Follows from the definition of \mathcal{S}^* . In fact, let $u(t) = 0$, for $t \in \{0, \dots, T-2\}$ and $u(T-1) \neq 0$. Then $x(T) = Ax(T-1) + Bu(T-1) = Bu(T-1) \in \text{Im}(B) \subseteq \mathcal{S}^*$.

(ii) \Rightarrow (i) Because $x(1) = Bu(0)$ and $y(1) = Cx(1) = 0$, we have $x(1) \in \text{Im}(B) \cap \text{Ker}(C) = \mathcal{S}_1 \cap \text{Ker}(C)$. Similarly,

$$x(2) \in A(\mathcal{S}_1 \cap \text{Ker}(C)) + \text{Im}(B) = \mathcal{S}_2,$$

and $x(2) \in \text{Ker}(C)$ since $y(2) = Cx(2) = 0$. Recursively:

$$x(1) \in \mathcal{S}_1 = \text{Im}(B), \text{ and} \quad (15a)$$

$$x(i) \in \mathcal{S}_i = A(\mathcal{S}_{i-1} \cap \text{Ker}(C)) + \text{Im}(B). \quad (15b)$$

Since \mathcal{S}_i converges to \mathcal{S}^* in at most n steps [2], we have that $x(\tau) \in \mathcal{S}^*$ for all $\tau \geq n$, which concludes the proof. ■

We are now ready to prove Theorem 2.

Proof of Theorem 2: From (10), when $x(0) = 0$, any state trajectory of length T that generates an identically zero output of length T can be parameterized with $\alpha = 0$ and $\beta \in \text{Ker}(YK_0)$. Using Lemma 3, the set \mathcal{S}^* can be equivalently written as the final states reached by such trajectories, that is, $\mathcal{S}^* = X_F K_0 \text{Ker}(YK_0)$, which concludes the proof. ■

Remark 2 (Obtaining \mathcal{R}^ from \mathcal{V}^* and \mathcal{S}^*):* The combined knowledge of \mathcal{V}^* and \mathcal{S}^* allows us to find \mathcal{R}^* as [2]

$$\mathcal{R}^* = \mathcal{V}^* \cap \mathcal{S}^*. \quad (16)$$

Remark 3 (Direct vs indirect invariant subspaces computation): A direct comparison between our formulas and classic

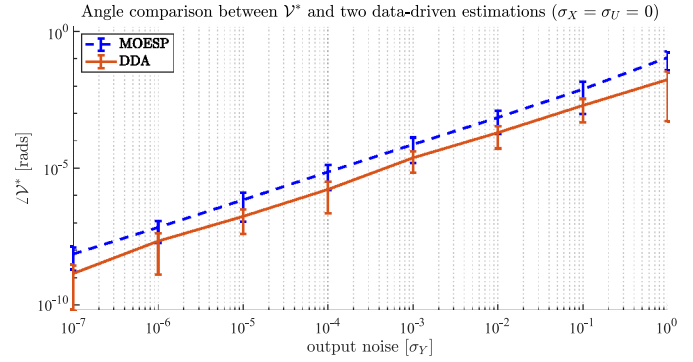


Fig. 1. This figure shows a comparison for computing \mathcal{V}^* with two different data driven approaches for minimal system [26, Example 6.6]. Outputs Y are collected with noise, i.e., $Y = \hat{Y} + \Delta_Y$, where Y is the measured data and Δ_Y is the noise matrix with i.i.d. entries, zero mean, and variance σ_Y . In blue (dashed) we show the result obtained through the MOESP algorithm (see [26]). In red (solid) we show the result obtained through the approach proposed in our paper (DDA). State trajectories X are assumed to be known only by MOESP, while DDA requires only X_0 . For every approach and for every value of σ_Y we perform a total of 100 Monte Carlo simulations and plot the mean value of the angle between the estimated and the model based \mathcal{V}^* (true subspace). $T = 50$ for MOESP, and $T = 3, N = 20$ for DDA.

indirect data-driven approaches is not straightforward. First, our formulas for \mathcal{V}^* and \mathcal{S}^* use data that is not sufficient to estimate the system matrices (e.g., the inputs U and the state trajectories X are not used in Theorems 1 and 2). Second, when inputs and outputs are available, system identification only provides the system matrices up to a similarity transformation. Hence, the subspaces computed with the identified matrices would not match the original subspaces since the similarity transformation remains unknown without state information. Third, system identification methods make assumptions (such as controllability and observability) that are not required for our approach. For example, let $A = \begin{bmatrix} 0.5 & 0 \\ 0 & 1 \end{bmatrix}$, $B = \begin{bmatrix} 1 \\ 0 \end{bmatrix}$, $C_1 = [3 \quad -5]$, and $C_2 = [3 \quad 4]$ where (A, B) is not controllable. We notice that $\Sigma_1 = (A, B, C_1)$ and $\Sigma_2 = (A, B, C_2)$ share the same input-output relationship, i.e., there exist input-output trajectories which are compatible with both systems. However, Σ_1 and Σ_2 do not share the same \mathcal{V}^* , in fact

$$\mathcal{V}_{\Sigma_1}^* = \begin{bmatrix} 1.00 \\ 0.60 \end{bmatrix}, \quad \mathcal{V}_{\Sigma_2}^* = \begin{bmatrix} 1.00 \\ -0.75 \end{bmatrix}.$$

System identification using input-output data cannot distinguish between Σ_1 and Σ_2 and, as a consequence, fails at estimating the correct invariant subspaces. Instead, our data-driven formulas work also in this situation.

Although a formal discussion of how noise affects the identification of subspaces is beyond the scope of this letter, in Fig. 1 we offer a qualitative comparison of how our approach performs with respect to a traditional system identification followed by a model based geometric approach. We observe that the tools presented in this letter are robust to noise. We refer to the image caption for the implementation details and to [25] for the code to reproduce this result.

The state of a system can be confined within a subspace \mathcal{V} through a state-feedback controller if and only if \mathcal{V} is a controlled invariant subspace. We continue this section with

the data-driven design of such state-feedback controller, that is, the data-driven design of a matrix F such that

$$(A + BF)\mathcal{V} \subseteq \mathcal{V}. \quad (17)$$

For a trajectory X_T and input U_T , let

$$X_{0,T} = [x(1) \quad x(2) \quad \cdots \quad x(T-1)], \quad (18a)$$

$$X_{1,T} = [x(2) \quad x(3) \quad \cdots \quad x(T)], \quad \text{and} \quad (18b)$$

$$U_{0,T} = [u(0) \quad u(1) \quad \cdots \quad u(T-1)]. \quad (18c)$$

Theorem 3 (Data-driven feedback for invariant subspace): Let X_T be the trajectory of (1) with input U_T and some initial condition. Let $\mathcal{V} = \text{Im}(V)$ be an $(A, \text{Im}(B))$ -controlled invariant subspace, and let

$$F = U_{0,T}X_{0,T}^\dagger + K\gamma, \quad (19)$$

with $K = \text{Ker}(X_{0,T})$ and

$$\gamma = -((I - VV^\dagger)X_{1,T}K)^\dagger (I - VV^\dagger)X_{1,T}X_{0,T}^\dagger VV^\dagger. \quad (20)$$

If $[U_{0,T}^\top \ X_{0,T}^\top]^\top$ is full-row rank,² then $(A + BF)\mathcal{V} \subseteq \mathcal{V}$.

Proof: From [15, Theorem 2], for any state-feedback gain F , the closed loop matrix can be written as

$$A + BF = X_{1,T}G,$$

where the matrix G satisfies $X_{0,T}G = I$ and $U_{0,T}G = F$. Further, F renders the subspace \mathcal{V} invariant if and only if $(A + BF)\mathcal{V} = X_{1,T}G\mathcal{V} \subseteq \mathcal{V}$, or, equivalently,

$$(I - VV^\dagger)X_{1,T}GV = 0,$$

where $V = \text{Basis}(\mathcal{V})$ and $(I - VV^\dagger)$ is a projector onto \mathcal{V}^\perp . From $X_{0,T}G = I$ we obtain $G = X_{0,T}^\dagger + K\gamma$, where γ is any matrix verifying the equality

$$(I - VV^\dagger)X_{1,T}(X_{0,T}^\dagger + K\gamma)V = 0.$$

Solving for γ (a solution γ exists because \mathcal{V} is an (A, B) -controlled invariant subspace and $[U_{0,T}^\top \ X_{0,T}^\top]^\top$ is full-row rank) and using $U_{0,T}G = F$ concludes the proof. ■

Theorem 3 details the computation of a feedback matrix that renders a subspace invariant, from sufficiently informative state and input trajectories. It should be noticed that Theorem 3 does not guarantee the internal, nor external, stability of the subspace, which imposes additional constraints on γ . This is left as a topic of future investigation.

To conclude this section we present a strategy to identify the invariant zeros of (1) from data. We make the assumption that (1) is such that \mathcal{R}^* is the trivial subspace. Systems with $\mathcal{R}^* \neq \{0\}$ are intrinsically vulnerable to, e.g., undetectable malicious attacks with unstable state trajectories. On the other hand, when $\mathcal{R}^* = \{0\}$, the existence of unstable invisible trajectories depends on the modulo of its invariant zeros. In fact, the knowledge of the number and magnitude of the invariant zeros when $\mathcal{R}^* = \{0\}$ is essential when studying problems such as noninteracting control [2] and attack detection [7], motivating our interest in their identification.

Theorem 4 (Data-driven invariant zeros): Let X and \mathcal{V}^* be as in (4a) and (9), respectively, with $T \geq n$. Let $V = \text{Basis}(\mathcal{V}^*)$

²This condition requires the trajectory to be sufficiently informative and is related to the notion of persistency of excitation [15], [21], [27].

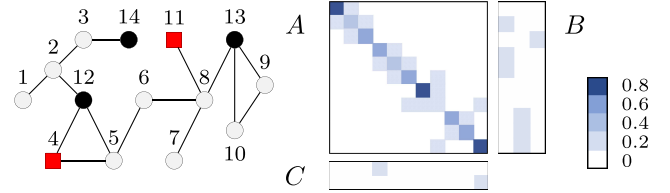


Fig. 2. An example of consensus network. On the left, agents are numbered from 1 through 14, where nodes {12, 13, 14} (in black) are the leaders and nodes {4, 11} (square) are the network monitors. On the right, the weighted adjacency matrix for the follower nodes {1, ..., 11} is shown, together with the input and output matrices (the numerical values of the entries of the matrices are color coded and belong to the set {0, 0.2, 0.4, 0.6, 0.8}).

and assume that $\mathcal{R}^* = \{0\}$. Then, $z \in \mathbb{C}$ is an invariant zero of (1) if and only if the matrix

$$\begin{bmatrix} XX^\dagger(I \otimes V) & -([z \ z^2 \ \cdots \ z^T] \otimes I)^\top \end{bmatrix} \quad (21)$$

has a nontrivial kernel.

Proof: When $\mathcal{V}^* \neq \{0\}$ and $\mathcal{R}^* = \{0\}$, there exists a trajectory $x(t) = z^t x(0)$, with $x(t) \in \mathcal{V}^*$ for all $t \geq 0$ and z an invariant zero of (1) [2]. We write such trajectory as

$$X_T^V = [(zI)^\top \ \cdots \ (z^T I)^\top]v = ([z \ \cdots \ z^T] \otimes I)^\top v. \quad (22)$$

With Assumption 1, any trajectory belongs to the image of the data matrix X . Then, when the trajectory X_T^V above exists, there also exists a vector $\bar{w} \in X^\dagger(I \otimes V)$ such that $X\bar{w} = X_T^V$. The condition on \bar{w} imposes that the trajectory is compatible with (1) while evolving inside \mathcal{V}^* . Both vectors $v \neq 0$ and $\bar{w} = X^\dagger(I \otimes V)w \neq 0$ exist if and only if

$$XX^\dagger(I \otimes V)w = ([z \ z^2 \ \cdots \ z^T] \otimes I)^\top v \quad (23)$$

i.e., the kernel of $[XX^\dagger(I \otimes V) \quad -([z \ z^2 \ \cdots \ z^T] \otimes I)^\top]$ is non-empty, concluding the proof. ■

The invariant zeros of the system (1) can be equivalently characterized using data collected as in (18).

Lemma 4 (Data-driven invariant zeros): Let \mathcal{V}^* be as in (9) and assume that $\mathcal{R}^* = \{0\}$. Let $T = [T_1 \ T_2]$, with $T_1 = \text{Basis}(\mathcal{V}^*)$, and T_2 chosen such that T is nonsingular. Finally, let $G = X_{0,T}^\dagger + K\gamma$, with γ defined as in (20). Then, the invariant zeros of (1) are the eigenvalues of A_{11} , where

$$T^{-1}(X_{1,T}G)T = \begin{bmatrix} A_{11} & A_{12} \\ 0 & A_{22} \end{bmatrix}. \quad (24)$$

Proof: This result derives from the facts that (i) the closed loop system with the state feedback $u = Fx$ satisfies

$$A + BF = X_{1,T}G, \quad (25)$$

(ii) the subspace \mathcal{V}^* is invariant for the closed-loop matrix $A + BF$, and (iii) the invariant zeros of (1) are the eigenvalues of the closed-loop matrix $A + BF$ contained in \mathcal{V}^* . ■

IV. MALICIOUS ATTACKS: AN ILLUSTRATIVE EXAMPLE

To illustrate a possible use of the theory we developed, consider the leader-follower consensus network in Fig. 2.

The network is equipped with two monitoring nodes, specifically, nodes 4 and 11. The state of the monitoring nodes is

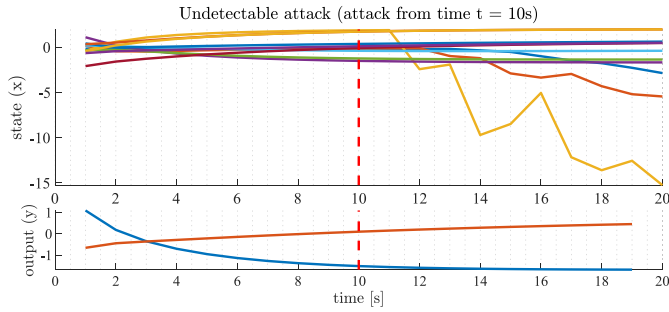


Fig. 3. In this figure we show an attack on the network of Fig. 2. The systems initial condition is chosen randomly and the leaders impose $u = [-2 \ 2 \ 4]^T$. The attacker waits for the system to reach its equilibrium and then, at time $t = 10s$, injects an attack A_T as proposed in Sec IV. We notice how the system state is perturbed from the equilibrium, while the output of the system remains unaffected by the attack, rendering the attack action effectively invisible at the output. We use the following parameters: time horizon $T = 49 > n$, and number of experimental trajectories $N = n + mT = 158$, with X_0 and U satisfying Assumption 1.

used to detect any anomalous behavior of the network from its nominal dynamics (see also [28]). We let an attacker take control of the leader nodes, and seek for an attack strategy that remains undetectable from the monitoring nodes, and leverages only historical data of the network dynamics. The attacker strategy is designed as follows: (i) compute \mathcal{V}^* and \mathcal{S}^* using Theorems 1 and 2, respectively, and find $\mathcal{R}^* = \mathcal{V}^* \cap \mathcal{S}^*$; (ii) for $R = \text{Basis}(\mathcal{R}^*)$, and X , U and K_0 defined as in (4a), (4e) and Assumption 1, compute $P_1 \neq 0$ as

$$\begin{bmatrix} XK_0 & I \otimes R \end{bmatrix} \begin{bmatrix} P_1 \\ P_2 \end{bmatrix} = 0; \quad (26)$$

and (iii) choose the attack input A_T as $A_T \in \text{Im}(UK_0P_1)$. Then, for any initial state $x(0)$ and nominal control input U_T , the output of (2)-(3) with input U_T is indistinguishable from the output with input $U_T + A_T$. As can be seen in Fig. 3 from time $t = 10s$, the attacker strategy perturbs the state of the network but does not affect the monitoring nodes, thus remaining undetectable. In fact, it can be shown that any input $A_T \in \text{Im}(UK_0P)$ moves the state trajectory within the controlled invariant $\mathcal{R}^* \subseteq \text{Ker}(C)$, thus affecting the state of the system but not its output.

V. CONCLUSION

In this letter we show how experimental data can be used to learn key invariant subspaces of a linear system. In particular, we derive data-driven expressions for \mathcal{V}^* , the largest $(A, \text{Im}(B))$ -controlled invariant contained in $\text{Ker}(C)$, and \mathcal{S}^* , the smallest $(A, \text{Ker}(C))$ -conditioned invariant containing $\text{Im}(B)$. Being able to identify these subspaces from data suggests that much of the results and intuitions of the geometric approach to control can be conveniently reworked in a data-driven framework. To support this point, we leverage the identified invariant subspaces to design a data-driven feedback controller to force the state inside a desired controlled invariant subspace, and to compute the invariant zeros of the system. Finally, as an example of the theoretical results, we design a data-driven undetectable attack. Applications and extensions of the proposed results are numerous, and are left as the subject of future investigation.

REFERENCES

- [1] K. J. Åström and R. M. Murray, *Feedback Systems: An Introduction for Scientists and Engineers*. Princeton, NJ, USA: Princeton Univ. Press, 2010.
- [2] G. Basile and G. Marro, *Controlled and Conditioned Invariants in Linear System Theory*. Englewood Cliffs, NJ, USA: Prentice-Hall, 1991.
- [3] I. Markovsky and P. Rapisarda, "Data-driven simulation and control," *Int. J. Control*, vol. 81, no. 12, pp. 1946–1959, 2008.
- [4] A. Isidori, *Nonlinear Control Systems*. (Communications and Control Engineering Series), 3rd ed. London, U.K.: Springer, 1995.
- [5] W. M. Wonham and A. S. Morse, "Decoupling and pole assignment in linear multivariable systems: A geometric approach," *SIAM J. Control*, vol. 8, no. 1, pp. 1–18, 1970.
- [6] M.-A. Massoumnia, G. C. Verghese, and A. S. Willsky, "Failure detection and identification," *IEEE Trans. Autom. Control*, vol. 34, no. 3, pp. 316–321, Mar. 1989.
- [7] F. Pasqualetti, F. Dörfler, and F. Bullo, "Attack detection and identification in cyber-physical systems," *IEEE Trans. Autom. Control*, vol. 58, no. 11, pp. 2715–2729, Nov. 2013.
- [8] H. Fawzi, P. Tabuada, and S. Diggavi, "Secure estimation and control for cyber-physical systems under adversarial attacks," *IEEE Trans. Autom. Control*, vol. 59, no. 6, pp. 1454–1467, Jun. 2014.
- [9] M. Gevers, "Identification for control: From the early achievements to the revival of experiment design," *Eur. J. Control*, vol. 11, nos. 4–5, pp. 335–352, 2005.
- [10] V. Krishnan and F. Pasqualetti, "On direct vs indirect data-driven predictive control," in *Proc. 60th IEEE Conf. Decis. Control*, Austin, TX, USA, Dec. 2021, pp. 736–741.
- [11] F. Dörfler, J. Coulson, and I. Markovsky, "Bridging direct & indirect data-driven control formulations via regularizations and relaxations," Jan. 2021, *arXiv:2101.01273*.
- [12] H. J. van Waarde, J. Eising, H. L. Trentelman, and M. K. Camlibel, "Data informativity: A new perspective on data-driven analysis and control," *IEEE Trans. Autom. Control*, vol. 65, no. 11, pp. 4753–4768, Nov. 2020.
- [13] G. Baggio, D. S. Bassett, and F. Pasqualetti, "Data-driven control of complex networks," *Nat. Commun.*, vol. 12, p. 1429, Mar. 2021.
- [14] N. Monshizadeh, "Amidst data-driven model reduction and control," *IEEE Contr. Syst. Lett.*, vol. 4, pp. 833–838, 2020.
- [15] C. De Persis and P. Tesi, "Formulas for data-driven control: Stabilization, optimality, and robustness," *IEEE Trans. Autom. Control*, vol. 65, no. 3, pp. 909–924, Mar. 2020.
- [16] A. Alilbhoj and J. Cortés, "Data-based receding horizon control of linear network systems," *IEEE Contr. Syst. Lett.*, vol. 5, pp. 1207–1212, 2021.
- [17] F. Celi, G. Baggio, and F. Pasqualetti, "Distributed learning of optimal controls for linear systems," in *Proc. IEEE Conf. Decis. Control*, Austin, TX, USA, Dec. 2021, pp. 5764–5769.
- [18] É. Garrabé and G. Russo, "On the design of autonomous agents from multiple data sources," *IEEE Contr. Syst. Lett.*, vol. 6, pp. 698–703, 2021.
- [19] J. Jiao, H. J. van Waarde, H. L. Trentelman, M. K. Camlibel, and S. Hirche, "Data-driven output synchronization of heterogeneous leader-follower multi-agent systems," in *Proc. IEEE Conf. Decis. Control*, Austin, TX, USA, Dec. 2021, pp. 466–471.
- [20] S. M. Turan and G. Ferrari-Trecate, "Data-driven unknown-input observers and state estimation," *IEEE Contr. Syst. Lett.*, vol. 6, pp. 1424–1429, 2021.
- [21] I. Markovsky and F. Dörfler, "Behavioral systems theory in data-driven analysis, signal processing, and control," *Annu. Rev. Control*, vol. 52, pp. 42–64, Jan. 2021.
- [22] D. S. Bernstein, *Matrix Mathematics*, 2nd ed. Princeton, NJ, USA: Princeton Univ. Press, 2009.
- [23] W. M. Wonham, *Linear Multivariable Control: A Geometric Approach*, 3rd ed. New York, NY, USA: Springer, 1985.
- [24] H. L. Trentelman, A. A. Stoorvogel, and M. Hautus, *Control Theory for Linear Systems*. London, U.K.: Springer, 2001.
- [25] "Data-Driven Geometric Approach to Control." [Online]. Available: <https://github.com/federicoceli/ddga> (Accessed: Apr. 15, 2022).
- [26] T. Katayama, *Subspace Methods for System Identification*. (Communications and Control Engineering). London, U.K.: Springer-Verlag, 2005.
- [27] J. C. Willems, P. Rapisarda, I. Markovsky, and B. L. M. De Moor, "A note on persistency of excitation," *Syst. Control Lett.*, vol. 54, no. 4, pp. 325–329, 2005.
- [28] F. Pasqualetti, A. Bicchi, and F. Bullo, "Consensus computation in unreliable networks: A system theoretic approach," *IEEE Trans. Autom. Control*, vol. 57, no. 1, pp. 90–104, Jan. 2012.